Progress in manufacturing the first 8.4 m off-axis segment for the Giant Magellan Telescope

H. M. Martin[a], J. H. Burge[a,b], B. Cuerden[a], W. B. Davison[a], J. S. Kingsley[a], W. C. Kittrell[a], R. D. Lutz[a], S. M. Miller[a], C. Zhao[b] and T. Zobrist[b]

[a]Steward Observatory, University of Arizona, Tucson, AZ 85721, USA
[b]College of Optical Sciences, University of Arizona, Tucson, AZ 85721, USA

ABSTRACT

The first of the 8.4 m off-axis segments for the primary mirror of the Giant Magellan Telescope is being manufactured at the Steward Observatory Mirror Lab. In addition to the manufacture of the segment, this project includes the development of a complete facility to make and measure all seven segments. We have installed a new 28 m test tower and designed a set of measurements to guide the fabrication and qualify the finished segments. The first test, a laser-tracker measurement of the ground surface, is operational. The principal optical test is a full-aperture interferometric test with a null corrector that includes a 3.75 m spherical mirror, a smaller sphere, and a computer-generated hologram. We have also designed a scanning pentaprism test to validate the measurement of low-order aberrations. The first segment has been cast and generated, and is in the process of loose-abrasive grinding.

Keywords: telescopes, optical fabrication, optical testing, aspheres, active optics

1. INTRODUCTION

The primary mirror for the Giant Magellan Telescope (GMT) consists of seven 8.4 m segments as shown in Figure 1.[1],[2] Each segment is a honeycomb sandwich mirror similar to the 8.4 m primary mirrors of the Large Binocular Telescope (LBT). They are the largest segments that can be made, and they guarantee a smooth wavefront over 8.4 m apertures. The GMT's secondary mirror is segmented to match the primary, with seven 1.1 m segments. The small and agile secondary segments perform the fine alignment for each 8.4 m subaperture. In the coherent mode of operation, the secondary segments are the deformable mirrors and perform the phasing of the 24.5 m aperture. While there is no easy way to achieve a coherent wavefront over such a large aperture, the GMT design is the simplest and most robust option available.

The GMT's simple yet powerful design is made possible by the ability to manufacture the 8.4 m primary mirror segments at the Steward Observatory Mirror Lab. Mechanically, the segments are similar to the LBT primary mirrors and allow use of mature technology for fabrication, support and thermal control.[3] The GMT segments do present a challenge because the outer, off-axis segments have 14 mm of aspheric departure. The asphericity is low-order, mostly astigmatism, and has little impact on fabrication, but it makes the measurement of the off-axis segments difficult and expensive. We have developed a set of measurements that supports the fabrication plan and assures excellent performance in the telescope. The measurements include a full-aperture, interferometric test with a unique non-axisymmetric null corrector, and an independent test of low-order aberrations that validates the accuracy of the null corrector. To guide loose-abrasive grinding and serve as a second independent measurement of low-order aberrations, we will use a laser tracker with additional stability references that improve the accuracy to 1 micron rms or better.

The development of the measurement systems is a major project in its own right. The principal optical test includes a 28 m test tower, a 3.75 m mirror as part of the null corrector, and novel use of computer-generated holograms and laser trackers as alignment tools. The tolerance analysis for this test includes a model of the full active optics system in the telescope, including alignment degrees of freedom as well as shape control. While the test system is not yet complete, a great deal of progress has been made. We have installed the new test tower, completed the 3.75 m mirror, and demonstrated important aspects of the alignment. Meanwhile, fabrication of the first off-axis segment has proceeded to loose-abrasive grinding of the optical surface.

Advanced Optical and Mechanical Technologies in Telescopes and Instrumentation, edited by Eli Atad-Ettedgui, Dietrich Lemke, Proc. of SPIE Vol. 7018, 70180C, (2008) · 0277-786X/08/$18 · doi: 10.1117/12.789805

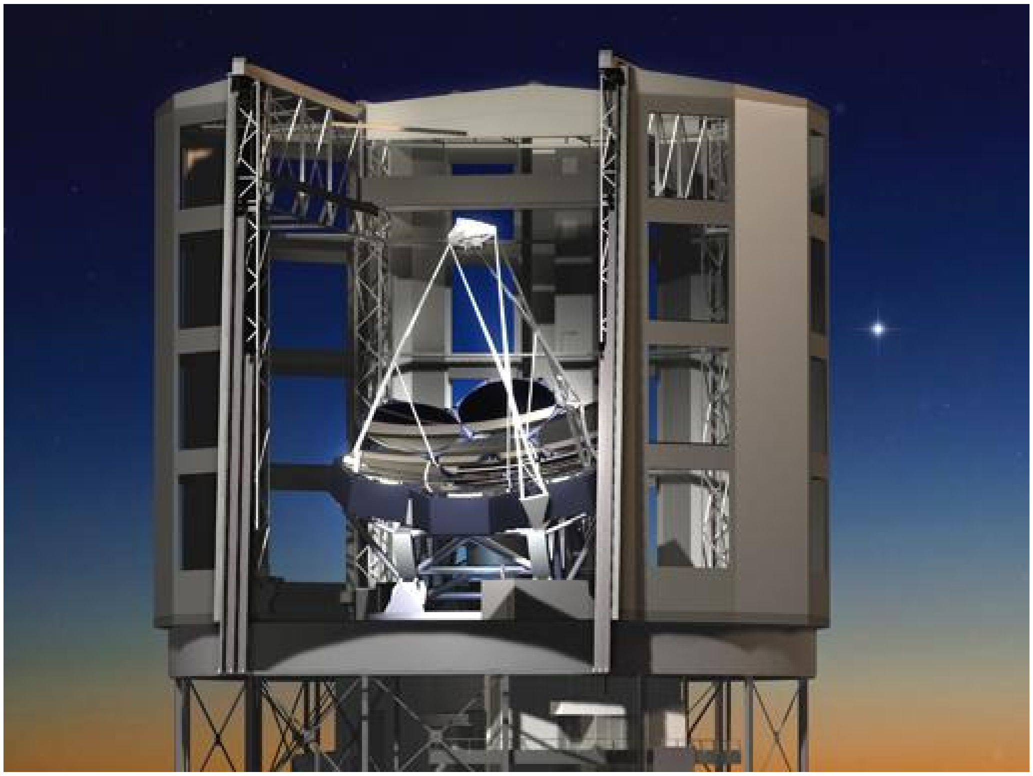

Figure 1. Model of the Giant Magellan Telescope. The seven primary mirror segments form a single parent surface, as do the seven matching secondary mirror segments.

The remainder of this paper describes all aspects of the manufacturing process and gives their status. Section 2 describes the design of the segment. Section 3 gives an overview of the manufacturing plan. Section 4 discusses the accuracy requirements for the segment. Section 5 describes the fabrication process and Section 6 describes the measurements. Section 7 presents the results of figuring and measuring the primary mirror for the off-axis New Solar Telescope at Big Bear Solar Observatory, whose surface is approximately a 1/5 scale model of the GMT segment. Section 8 summarizes the paper.

2. DESIGN OF THE SEGMENT

We have presented the mechanical design of the GMT segments previously.[3] The honeycomb sandwich mirror is much stiffer, yet lighter, than a comparable solid mirror. Gravitational deflections are reduced, and sensitivity to wind and support errors are greatly reduced. The lightweight structure and thin glass sections, combined with forced-air ventilation, reduce the mirror's thermal time constant to less than one hour, so neither thermo-elastic deflections nor mirror seeing makes a significant contribution to image blurring.

The optical design is nearly parabolic with R = 36 m and k = -0.9983. The off-axis distance is 8.71 m to the mechanical center of the segment.

3. MANUFACTURING PLAN

The manufacture of the first off-axis segment includes developing a complete facility for making all the segments. The greatest investment is the set of measurements needed to guide fabrication and guarantee accuracy. The principal optical test is a full-aperture interferometric measurement, with a non-axisymmetric null corrector that is larger than the mirror under test.[4],[5] Alignment tolerances for the null corrector are about 10 parts per million, difficult to achieve in a non-axisymmetric system. In order to guarantee the accuracy of the segment, we require an independent measurement of the segment's parameters that are sensitive to misalignments of the principal test. We provide this in the form of a scanning pentaprism test, whose sensitivity to low-order aberrations is about the same as that of the principal test.[6],[7] To guide the loose-abrasive grinding and initial polishing, we use a laser tracker with special stability references to monitor rigid-body motion and refractive index variations.[6],[8]

Apart from the measurements, fabrication of the segments is fairly straightforward, following the same procedures used for the MMT, Magellan and LBT primary mirrors.[9]-[11] Spin-casting creates the honeycomb sandwich structure with an accuracy of a few mm. The mirror is diamond-generated (machined) to define all critical external surfaces and bring the optical surface to an accuracy of about 10 micron rms. Loose-abrasive grinding and polishing of the optical surface are done with a stressed-lap polishing tool that actively conforms to the aspheric surface, augmented by small tools for local figuring.

The fabrication of the first segment is paced by development of the test systems. The remaining segments will flow through the lab without interruptions. The Mirror Lab has two 8.4 m capacity machines, one of which is generally used for generating and one for polishing. We believe the facility can produce finished segments at a rate exceeding one per year.

4. ACCURACY REQUIREMENTS

Accuracy requirements for the off-axis segments involve some considerations that do not apply to a symmetric telescope mirror. Requirements on small scales—up to about 2 m—are similar to those for a symmetric mirror, but there are several differences that affect the large-scale accuracy requirements for off-axis segments, essentially the requirements for control of low-order aberrations. First, power must be controlled to high accuracy in order to make the radii of curvature of the seven segments match. Second, certain low-order aberrations are more difficult to measure because of the lack of symmetry. Third, in addition to the usual active optics system that controls low-order aberrations by bending the mirror, the off-axis segment has two alignment degrees of freedom for in-plane motion—off-axis distance and clocking angle—that affect low-order aberrations and will be adjusted in the telescope.

We make use of the active optics, including alignment, in setting the accuracy requirements for manufacture of the segments. Alignment errors in the test will cause significant uncertainty in several low-order aberrations. Ultimately, these aberrations will be measured to high accuracy in the telescope with a wavefront sensor, and the aberrations will be adjusted both by shifting the position of the segment in the telescope and by bending it with the active supports. The fundamental requirement for the lab measurement is therefore to measure all aberrations to sufficient accuracy that the errors can be corrected in the telescope by a combination of shifting the position of the segment and bending it, with limits on the displacement of the segment and the actuator forces to bend it. It costs almost nothing to correct manufacturing errors with the active optics system in the telescope. They are fixed errors that will be corrected transparently during the initial optimization of the segment's alignment and support forces.

Optical specifications for the GMT segment are listed in Table 1. These specifications apply to the combination of polishing and measuring errors, after active correction of low-order aberrations by displacing and bending the segment in the telescope. These active corrections are limited to maximum displacements of 2 mm in off-axis distance and 50 arcseconds in clocking, and maximum correction forces of 42 N rms.

The figure specification is a structure function defined by the parameters listed in Table 1. A structure function is a measure of the wavefront error as a function of spatial scale and is defined as the mean square wavefront difference between points in the aperture as a function of their separation. We use this form of specification because the wavefront errors caused by the atmosphere are commonly described by a structure function with a power law form and amplitude defined by the coherence length r_0. The segment specification is tightened on large scales in a way that corresponds to removal of tilt by rapid active guiding, and relaxed on small scales to allow a small fraction of light to be scattered outside the core of the point-spread function. We generally plot the square root of the structure function or rms wavefront difference, shown in Figure 2.

Table 1. Optical specifications for the first GMT segment

parameter	specification	goal
geometry		
radius of curvature R	36,000.0 $\pm$ 1.0 mm	$\pm$ 0.3 mm
measurement accuracy for R	$\pm$ 0.5 mm	$\pm$ 0.3 mm
conic constant k	-0.998286	
off-axis distance	8710 $\pm$ 2 mm	$\pm$ 1 mm
clocking angle	$\pm$ 50 arcseconds	
figure (structure function, λ = 500 nm)		
clear aperture	8.365 m	
coherence length r_0	91.9 cm	
scattering loss	< 2.0%	< 1.5%

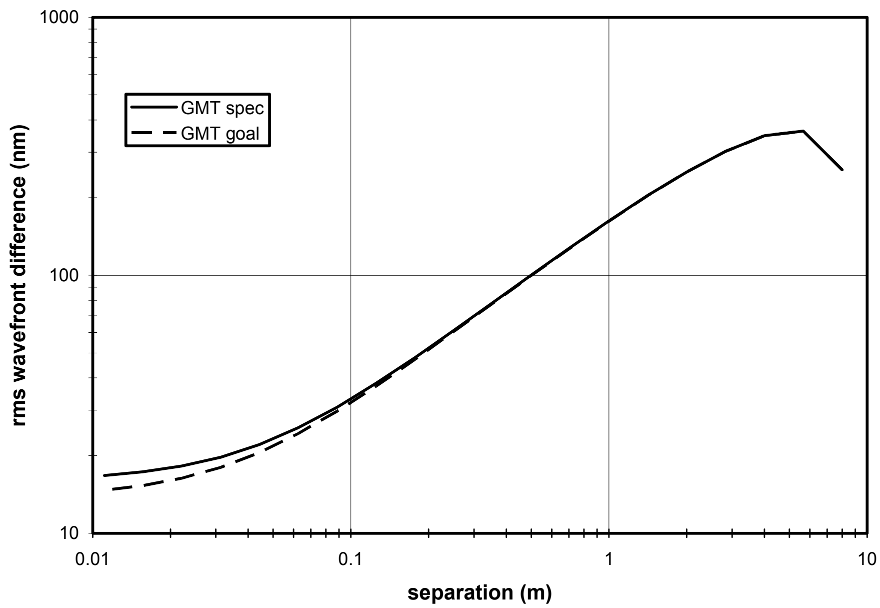

Figure 2. Figure specification for the GMT segment. The curve is the square root of the structure function. The goal with 1.5% scattering loss is also shown.

The optical specification includes tight tolerances on off-axis distance and clocking angle (rotation of the segment about its mechanical axis) in order to limit displacements of the segments relative to their cells, which are fixed in the telescope. There is also a tight requirement for matching radius of curvature among all seven segments, primarily to provide equal plate scales for imaging over the 20 arcminute field. The segments' radii must match well enough in the lab that they can be adjusted—using a combination of displacement and bending—to give essentially a perfect match in the telescope. In order to achieve this level of matching, the radius of curvature must be measured to an accuracy of ±0.5 mm with a goal of ±0.3 mm. The radius measurement must be stable and repeatable to ±0.3 mm over the period of manufacture of all the GMT segments.

There is no explicit tolerance on conic constant. Any error in conic constant is considered a figure error.

Compensation for low-order aberrations by displacement and bending depends on the sensitivity of those aberrations to displacements and correction forces. Only focus, astigmatism and coma depend strongly on the position of the segment. Their sensitivities to radial displacement and clocking are listed in Table 2. These displacements are along the surface of the parent ellipsoid. A small displacement perpendicular to the radial direction produces the same aberrations as clocking.

Table 2. Sensitivity of low-order aberrations to radial shift and clocking angle

aberration	rms surface error (nm)	
	1 mm radial shift	50" rotation
focus	800	
astigmatism	540	1280
coma	50	170

The sensitivities of these aberrations to segment position are coupled, so they cannot be corrected independently. For any combination of aberrations, however, there is an optimum adjustment of the segment position that minimizes the rms wavefront error. This is not exactly the adjustment we want, because we will use the actuators to bend out the residual low-order aberrations and we must keep track of actuator forces as well as residual errors. We choose to optimize the adjustment of segment position so that the rms actuator force is minimized.

Table 3 gives the relationship between surface error and correction force for a number of low-order aberrations. It also lists the residual surface errors after correction, and the amplitude of each aberration that can be corrected with 10 N rms force. The forces and residual errors were calculated by finite element analysis. We have verified similar calculations for the LBT primary mirrors by applying correction forces and measuring the figure change in the lab.

Table 3. Correction forces and residual errors for five low-order aberrations. Each aberration is given an amplitude of 1 micron rms surface.

aberration	correction force	residual error after correction	amplitude that can be corrected with 10 N rms force
	N rms	nm rms	nm rms
focus	35	54	290
astigmatism	12	18	830
coma	140	140	71
trefoil	55	45	180
spherical aberration	390	280	26

The correction forces are applied as a set of bending modes, starting with the softest mode that is similar to astigmatism and going to increasingly stiffer modes. The number of modes is limited and we do not approach independent control of all 165 actuators, with unreasonably large forces. The correction forces and residual errors depend on the number of bending modes used to correct each aberration. Using more modes increases the correction force and decreases the residual error. For each aberration, only certain modes have the right symmetry, so the ranges of possible correction forces and residual errors contain only a few discrete values. Table 3 reflects a reasonable balance between forces and residual errors, but other combinations could be used.

Large amounts of astigmatism can be corrected with low forces and residual errors. Focus is a somewhat stiffer aberration while coma is much stiffer. Spherical aberration is very stiff, but it is relatively insensitive to alignment errors in the optical test. The types of errors that would cause spherical aberration in a symmetric mirror cause astigmatism and coma in the off-axis segments.

The allowed correction force (42 N rms) must accommodate not only uncertainty in the lab measurements, but also figure errors that are measured in the lab but not polished out of the segment. As a preliminary budget for correction force, we allocate 30 N rms to relax the fabrication tolerance and 30 N rms to allow for uncertainties in the measurement. In other words, the as-measured figure must be correctable with 30 N rms forces, and the uncertainty in figure due to measurement errors must be correctable with 30 N rms forces.

5. FABRICATION

5.1 Status of the first segment

The first segment was spin-cast, with a best-fit symmetric parabolic surface, in July 2005. We generated and polished the flat rear surface, and bonded the load spreaders that are the interfaces to the telescope support actuators. Fabrication was interrupted for erection of the new test tower in late 2006 and early 2007. We then generated the front surface, introducing the 14 mm aspheric departure, and started loose-abrasive in March 2008. We are testing the laser tracker system that will measure the ground surface and guide the fabrication until we have a polished surface suitable for the principal optical test.

5.2 Generating

The segment was machined, or generated, using a computer-controlled mill (the Large Optical Generator, or LOG) that has been used to generate all large aspheric mirrors at the Mirror Lab. In our standard generating technique, the mirror rotates slowly on a turntable while the tool moves slowly along a profile $z(r)$ from edge to center, producing a spiral-shaped cut on the mirror. The off-axis segment requires a modification to this method. We have nowhere near the capacity to mount the segment off-axis and do an axisymmetric cut, and this is not necessary with 3-axis control of the machine. We mount the segment centered on the turntable, as shown in Figure 3, and adjust the tool position as a function of the segment's rotation angle.

The most straightforward modification of the standard tool path would be to add vertical motion as a function of segment rotation angle to create the aspheric shape. We were concerned about backlash in the tool motion, which would be imprinted on the surface. In order to minimize the effect of backlash, we maintain a monotonic vertical motion and weave in the horizontal direction instead, making the tool essentially follow contours of constant height on the aspheric surface, superposed on the spiral path. Because the maximum slope on the segment's surface is 1:9, the effect of horizontal backlash is reduced by a factor of 9 or more.

We calibrate the LOG by measuring its tool motion with a laser tracker and creating a look-up table of corrections. The shape of the cut surface is also affected by tool wear and deflection of the segment support on the turntable. We measured the surface with a laser tracker and a profilometer, and made additional corrections to the tool path based on the measurements.

5.3 Loose-abrasive grinding and polishing

After completing the generating, we started loose-abrasive grinding in March 2008. Most of the loose-abrasive grinding and polishing will be done with a 1.2 m stressed lap, shown in Figure 4. The stressed lap's aluminum plate is bent elastically by computer-controlled actuators to follow the changing curvature of the aspheric surface as it moves over that surface. This allows use of a large, stiff tool with a strong smoothing action. The lap is faced with pitch and, for loose-abrasive grinding, a layer of ceramic tiles. For figuring on small scales, we will also use an orbital polisher with compliant passive tools of 10 to 40 cm diameter.

The stressed-lap system works for off-axis as well as symmetric aspheres. Its ability to fit an aspheric surface is determined by the magnitude and type of shape changes across the surface. The GMT segment has 10 times the aspheric departure of an LBT mirror, but the shape is mostly astigmatism as opposed to spherical aberration, and the shape changes over the 1.2 m lap are much more benign. The magnitude of lap bending for a GMT segment is slightly greater than that for the Magellan and LBT mirrors, but the forces required to bend the plate are slightly less for GMT.

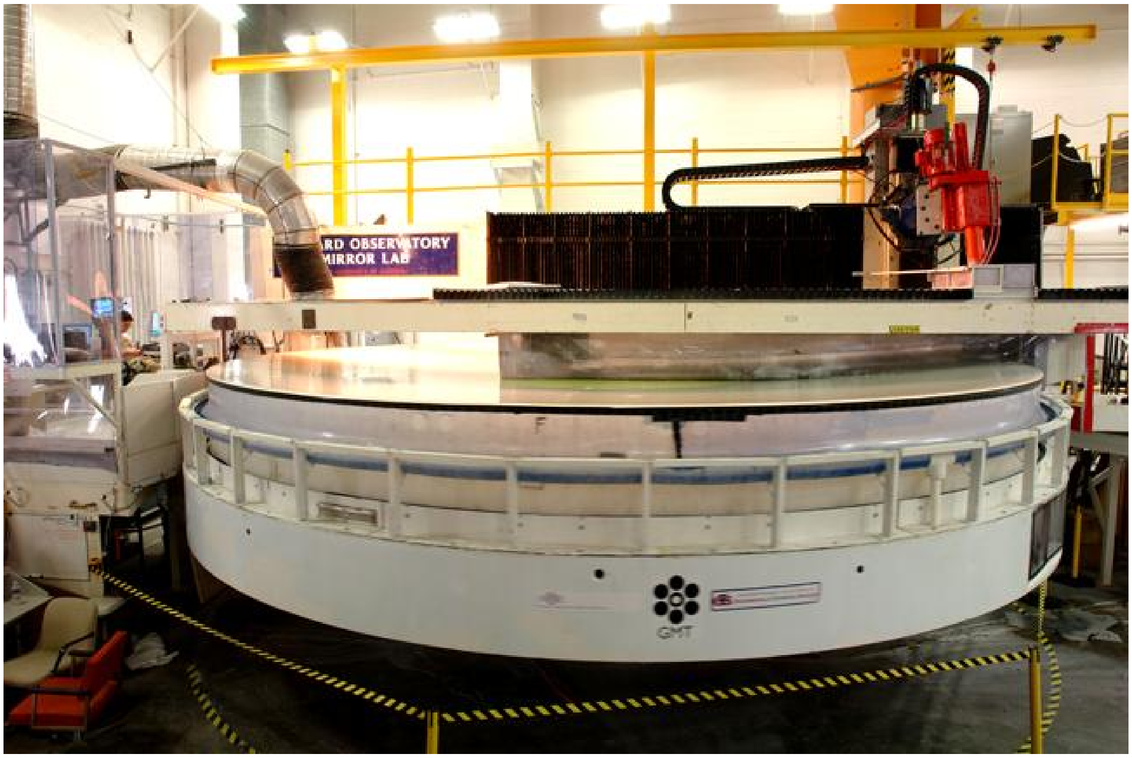

Figure 3. First GMT off-axis segment being diamond-generated on the Large Optical Generator. The path of the diamond wheel (at the end of the red spindle) is loosely enclosed in plastic in order to contain the coolant and ground glass.

Figure 4. First day of loose-abrasive grinding the GMT segment with a 1.2 m stressed lap. This work is done on the Large Optical Generator shown in Figure 3, but converted to a polishing machine. A second 8.4 m polishing machine will be used for final figuring.

The only significant change in the stressed-lap system for the GMT segment, or any off-axis mirror, is a change in the control software. For a symmetric mirror, the lap's shape is a function of its distance from the center of the mirror r and its rotation angle θ. Both variables are measured directly with encoders on the polishing machine; the machine's cylindrical polar coordinate system is the same as the mirror's. Commands for the lap's bending actuators are determined by empirically optimizing the lap shape for a coarse grid of lap positions (r, θ) and interpolating from that grid onto a fine two-dimensional look-up table, which is accessed in real time during polishing.

For an off-axis mirror, the mirror is centered on the polishing machine's turntable, just as it is for generating. The lap shape is still a function of two variables, but now they are measured in the parent coordinate system: r represents the lap's distance from the optical axis of the parent and θ represents the lap's rotation angle with respect to a vector pointing from the lap to the parent axis. These variables are not measured directly by the machine's encoders, but they can be calculated from three encoder readings: lap horizontal position, lap rotation angle, and segment rotation angle. We calibrate the bending actuators in the same way we do for a symmetric mirror, optimizing the lap shape for a set of positions (r, θ) in parent coordinates. We could interpolate the commands onto a three-dimensional look-up table (where the three dimensions correspond to the machine's coordinate axes) and access it with direct encoder readings in real time. We choose instead to do the transformation from machine coordinates to parent coordinates in real time, and use the two-dimensional look-up table. The additional computations have no significant effect on performance.

Since the segment is centered on the turntable, we figure it as if it were axisymmetric. Most polishing strokes are axisymmetric when viewed from above, and the 14 mm of non-axisymmetric vertical motion is not readily apparent. The non-axisymmetric shape variations of the lap are also small enough that they can't be seen. A casual observer watching the polishing cannot tell that the mirror is off-axis.

To correct figure errors that are symmetric with respect to the center of the segment, we use polishing strokes with constant mirror rotation, and vary the lap's rotation rate and horizontal speed as a function of its horizontal position. We have several methods of correcting non-axisymmetric figure errors:

1. Vary the polishing pressure dynamically as a function of mirror rotation angle (increasing removal rate over high regions).
2. Vary the mirror rotation rate dynamically as a function of mirror rotation angle (increasing dwell time over high regions).
3. Have the mirror rotation oscillate between fixed angles (polishing exclusively on high regions).

The first method is used only with the stressed lap, while the other two methods can be used with the stressed lap or the orbital polisher.

6. MEASUREMENT

The set of measurements of the GMT segments has several high-level requirements:

1. Measure large-scale errors accurately enough that they can be corrected in the telescope with a combination of segment displacements within the specified position tolerance and bending using correction forces within the specified limit.
2. Measure small-scale errors to an accuracy that represents a small fraction of the specification for figure errors.
3. Measure the segment's geometry (radius of curvature, off-axis distance, and clocking angle) within the specified tolerances.
4. Include sufficient redundancy to make it very unlikely that a mistake in implementing one of the tests could cause a serious figure error.
5. Support all three stages of fabrication: generating, loose-abrasive grinding and polishing.

We are building a set of measurements that meet these requirements. They are presented in detail elsewhere in these proceedings.[5],[7],[8] The principal optical test is a full-aperture, high-resolution measurement of the figure, made by phase-shifting interferometry with a null corrector to compensate for the aspheric surface. Figure 5 shows the layout of the principal test. The null corrector comprises two spherical mirrors and a computer-generated hologram, that together transform the interferometer's spherical wavefront into a template wavefront for the off-axis segment. Most of the compensation is made by an oblique reflection off a 3.75 m spherical mirror. We measure the figure of this fold sphere *in situ* from its center of curvature, and correct for its figure error. A similar reflection off a 0.76 m sphere makes further compensation, and the hologram is designed to eliminate the residual error.

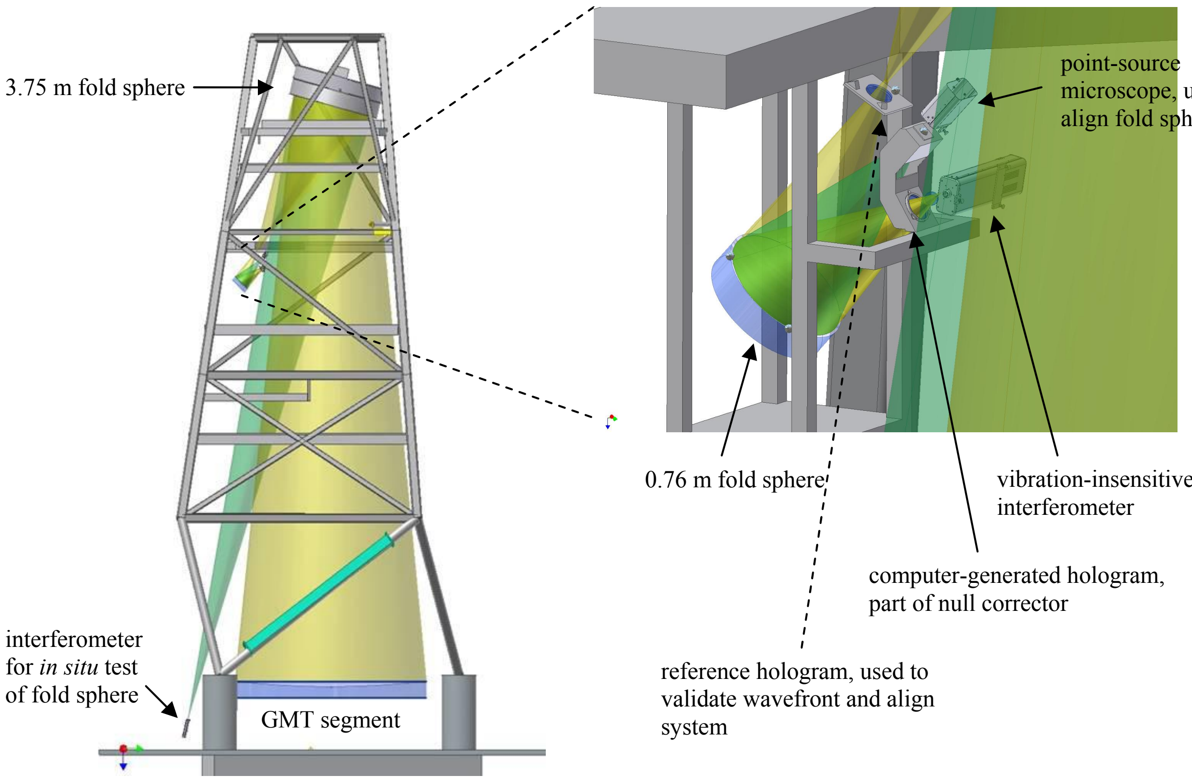

Figure 5. Model of the principal optical test for the GMT off-axis segments. At right is a close-up view of the interferometer and first two elements of the null corrector. Gold light cones represent the measurement of the GMT segment. Green light cones represent center-of-curvature measurements of the two fold spheres.

Alignment of the large null corrector is challenging. Tolerances are on the order of 10 microns for the interferometer, hologram and small fold sphere, and on the order of 100 microns for the larger dimensions involving the large fold sphere and the GMT segments. We have developed methods of alignment using holograms and laser trackers that will give the required accuracies. In addition to the main hologram that is part of the null corrector, we can insert a reference hologram into the beam, as shown in Figure 5, that serves two functions. First, it returns light to the interferometer to verify the accuracy of the wavefront produced by the main hologram and the small fold sphere. Second, it serves as an optical and mechanical reference to that wavefront, a reference that can be measured with a laser tracker. Combining this with laser tracker measurements of the large fold sphere and the GMT segment provides the measurements necessary to align the system.

We use a scanning pentaprism test to provide an independent measurement of low-order aberrations. This test, shown in Figure 6, measures slope errors in a number of one-dimensional scans across the surface. A narrow collimated beam, parallel to the optical axis of the parent, is scanned across the surface while a detector at the segment's focus monitors the position of the spot formed there. The spot displacements, proportional to the slope errors on the surface, are fit to a model to determine the low-order aberrations.

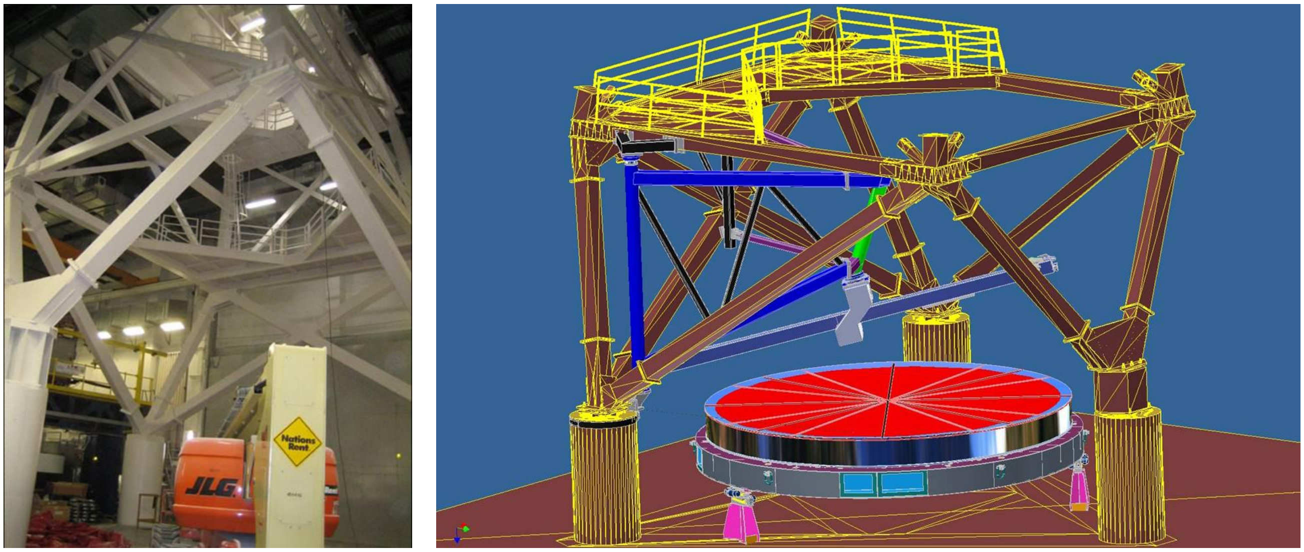

Figure 6. Left: Optical test tower at the Mirror Lab. Right: Model of the rail for the scanning pentaprism test, supported in the test tower. The pentaprism system is deployable and can rotate to any orientation in a plane perpendicular to the parent's optical axis. The pentaprism system includes a detector at the prime focus, which is about 18 m above the segment, above the model shown at right and near the top of the photo at left.

The third test uses a laser tracker to scan the surface. The laser tracker combines a distance-measuring interferometer with angular encoders and a tracking servo to follow a moving retroreflector and measure its position in three dimensions. The tracker is mounted on a fixed platform above the mirror while the retroreflector is scanned over the surface. Separate distance-measuring interferometers monitor rigid-body motion of the segment or laser tracker, as well as large-scale variations in refractive index. This test supports generating and loose-abrasive grinding, and provides an independent measurement of radius of curvature and astigmatism at roughly the level of the specification.

Finally, we will perform a shear test using the principal optical test. We will shift the segment ± 0.5 m about the parent optical axis to distinguish between small-scale errors on the segment surface and errors in the principal test.

Table 4 summarizes the tests of the GMT segments. All the tests use the new 28 m test tower, shown in Figure 6. It is taller, wider, stiffer and more versatile than the previous tower, in order to accommodate the GMT tests and tests of the primary and tertiary mirrors for the Large Synoptic Survey Telescope, as well as future mirrors with a range of focal lengths. The laser tracker measurement system is operational. We are making the components of the principal test, including the 3.75 m fold sphere, which was recently completed to an accuracy of better than 20 nm rms surface over its clear aperture. We recently completed the design of the pentaprism system.

7. MANUFACTURE OF THE NST PRIMARY MIRROR

Much of the critical technology for the off-axis GMT segments has been developed and demonstrated on a smaller scale through the manufacture of the 1.7 m off-axis primary mirror for the New Solar Telescope (NST) at Big Bear Solar Observatory.[12] This mirror, with a radius of 7.7 m and an off-axis distance of 1.84 m, is approximately a 1/5 scale model of a GMT segment. We figured the NST mirror with a 30 cm stressed lap and passive laps to an accuracy of 16 nm rms surface over its 1.6 m clear aperture. The optical test used a computer-generated hologram as a null corrector to compensate for the mirror's 2.7 mm of aspheric departure.

We also performed a scanning pentaprism test to validate the measurement of low-order aberrations. By rotating the pentaprism rail to four orientations in the plane perpendicular to the parent axis, we were able to measure astigmatism, coma, trefoil and spherical aberration. For all aberrations measured, the pentaprism results agreed with the interferometric test within the predicted uncertainties of the pentaprism measurement, which ranged from 8 nm rms surface for spherical aberration to 35 nm rms for trefoil.

Table 4. Overview of the measurements of the GMT surface

Test	Function	Purpose	Performance
Principal optical test Full-aperture interferometric test	Measure entire surface with 2 cm spatial resolution	Guide polishing, qualify finished surface	Low order: correctable with <25 N rms actuator force Higher order: <30 nm rms surface irregularity
Scanning pentaprism measurement	Measure surface errors corresponding to lowest bending modes	Redundant test for low-order shape, including radius of curvature	Lowest order modes: correctable with <20 N rms actuator force
Laser tracker (plus stability references)	Measure surface with ~60 cm spatial resolution	Guide coarse figuring Redundant test of shape	2 µm rms error per point 0.5 µm rms goal
Shear test using principal optical test	Shift mirror to allow separation of test errors from mirror features	Redundant test of high order figure errors	<30 nm rms

8. SUMMARY

We have made substantial progress in the manufacture of the first off-axis segment of the GMT primary mirror, including development of critical infrastructure that enables the efficient manufacture of all the segments. The largest and most expensive components of the principal optical test—the tower and the large fold sphere—are complete, and the techniques for aligning this test are well defined. Of the additional tests, the laser tracker measurement is working and the pentaprism test has a completed design. All preliminary work on the segment is complete, and it is ready to be figured as soon as the principal test is assembled.

REFERENCES

[1] M. Johns, "The Giant Magellan Telescope (GMT)", in *Ground-based and Airborne Telescopes*, ed. L. M. Stepp, Proc. SPIE 6267 (2006).

[2] M. Johns, R. Angel, S. Shectman, R. Bernstein, D. Fabricant, P. McCarthy and M. Phillips, "Status of the Giant Magellan Telescope (GMT) Project", in *Ground-based Telescopes*, ed. J. M. Oschmann, Proc. SPIE 5489, p. 441 (2004).

[3] H. M. Martin, J. R. P. Angel, J. H. Burge, B. Cuerden, W. B. Davison, M. Johns, J. S. Kingsley, L. B. Kot, R. D. Lutz, S. M. Miller, S. A. Shectman, P. A. Strittmatter and C. Zhao, "Design and manufacture of 8.4 m primary mirror segments and supports for the GMT", in *Optomechanical Technologies for Astronomy*, ed. E. Atad-Ettedgui, J. Antebi and D. Lemke, Proc. SPIE 6273 (2006).

[4] J. H. Burge, L. B. Kot, H. M. Martin, R. Zehnder, C. Zhao, "Design and analysis for interferometric measurements of the GMT primary mirror segments", in *Optomechanical Technologies for Astronomy*, ed. E. Atad-Ettedgui, J. Antebi and D. Lemke, Proc. SPIE 6273 (2006).

[5] J. H. Burge, W. Davison, C. Zhao and H. M. Martin, "Development of surface metrology for the Giant Magellan Telescope primary mirror", in *Advanced Optical and Mechanical Technologies in Telescopes and Instrumentation*, ed. E. Atad-Ettedgui and D. Lemke, Proc. SPIE 7018 (2008).

[6] J. H. Burge, L. B. Kot, H. M. Martin, C. Zhao, T. Zobrist, "Alternate surface measurements for GMT primary mirror segments", in *Optomechanical Technologies for Astronomy*, ed. E. Atad-Ettedgui, J. Antebi and D. Lemke, Proc. SPIE 6273 (2006).

[7] P. Su, J. H. Burge, B. Cuerden and H. M. Martin, "Scanning pentaprism measurements of off-axis aspherics", in *Advanced Optical and Mechanical Technologies in Telescopes and Instrumentation*, ed. E. Atad-Ettedgui and D. Lemke, Proc. SPIE 7018 (2008).

[8] T. Zobrist, J. H. Burge, W. Davison and H. M. Martin, "Measurement of large optical surfaces with a laser tracker", in *Advanced Optical and Mechanical Technologies in Telescopes and Instrumentation*, ed. E. Atad-Ettedgui and D. Lemke, Proc. SPIE 7018 (2008).

[9] B. H. Olbert, J. R. P. Angel, J. M. Hill and S. F. Hinman, "Casting 6.5-meter mirrors for the MMT conversion and Magellan", in *Advanced Technology Optical Telescopes V*, ed. L. M. Stepp, Proc. SPIE 2199, p. 144 (1994).

[10] H. M. Martin, R. G. Allen, J. H. Burge, L. R. Dettmann, D. A. Ketelsen, S. M. Miller and J. M. Sasian, "Fabrication of mirrors for the Magellan Telescopes and the Large Binocular Telescope", in *Large Ground-based Telescopes*, ed. J. M. Oschmann and L. M. Stepp, Proc. SPIE 4837, p. 609 (2003).

[11] H. M. Martin, R. G. Allen, B. Cuerden, J. M. Hill, D. A. Ketelsen, S. M. Miller, J. M. Sasian, M. T. Tuell and S. Warner, "Manufacture of the second 8.4 m primary mirror for the Large Binocular Telescope", in *Optomechanical Technologies for Astronomy*, ed. E. Atad-Ettedgui, J. Antebi and D. Lemke, Proc. SPIE 6273 (2006).

[12] H. M. Martin, J. H. Burge, S. M. Miller, B. K. Smith, R. Zehnder and C. Zhao, "Manufacture of a 1.7 m prototype of the GMT primary mirror segments", in *Optomechanical Technologies for Astronomy*, ed. E. Atad-Ettedgui, J. Antebi and D. Lemke, Proc. SPIE 6273 (2006).